Supporting Information

He et al. 10.1073/pnas.1404140111

SI Materials and Methods

Model of Oxygen-Induced Retinal Blood Vessel Regression and Quantification of Avascular Area. The model of oxygen-induced retinal blood vessel regression (OIR) was performed as described (1, 2). C57BL6 mice injected intravitreally (500 ng per eye) at postnatal day 7 (P7) with PDGF-CC (100-00CC; PeproTech; endotoxin level < 0.1 ng/μg), PDGF-AA (100-13A; PeproTech; endotoxin level < 0.1 ng/μg), PDGF-BB (100-14B; PeproTech; endotoxin level < 0.1 ng/μg), PDGF-DD (1159-SB; R&D; endotoxin level <0.01 EU/μg), or BSA as control were exposed to hyperbaric oxygen (75%) for 1 d or 5 d to induce retinal vasculature regression. After 5 d of hyperoxic stimulation, the mice were returned to room air for another 5 d. For the PDGF-CC/PDGF receptor (PDGFR) blocking assay in the OIR model, PDGFR-α (2 μg per eye; AF1062; R&D) or PDGFR-β (2 μg per eye; Novus Biologicals) or PDGF-CC neutralizing antibody (2 μg per eye; AF1447; R&D) with PDGF-CC (500 ng per eye) was injected into mouse vitreous at P7. The retinae were harvested for real-time PCR, Western blot, whole mounts, and cryosection staining. The retinal avascular areas were analyzed using retinal whole mounts stained with isolectin B4 (IB4) conjugated with Alexa Fluor 488 (Invitrogen) (1:200). Image analysis was performed using an A1 Imager and AxioVision software (Carl Zeiss). Avascular areas were outlined using ImageJ software (National Institutes of Health) and were quantified and presented as the percentage of the total area of the retina.

Measurement of Endotoxin Levels. In addition to the information provided by the manufacturers' datasheets, the endotoxin levels of the PDGF proteins also were measured using a Limulus Amebocyte Lysate test (QCL-1000; BioWhittaker, Inc.) according to the manufacturer's instructions. Mean OD readings obtained from duplicate wells were used. We found that the endotoxin level is <0.065 EU/μg in PDGF-AA, <0.044 EU/μg in PDGF-BB, <0.033 EU/μg in PDGF-CC, and is undetectable in PDGF-DD (Fig. S8*C*).

***Pdgf-c*–Deficient Mice.** The *pdgf-c*–deficient mice were described previously (3). The *pdgf-c*–deficient mice were bred onto C57BL6 background for more than six generations. Even though the *pdgf-c*–deficient mice were postnatal lethal on a 129 background (3), they survive and appear relatively normal on a C57BL6 background. The primers used for the genotyping PCR were 5′-CTG ATG TTC TCG TGA CTC TGA-3′; 5′-TAG CTA GTC GAT ACC GTC GA-3′; 5′-AGC TGA CAT TTG ATG AGA GAT-3′; and 5′-AGT AGG TGA AAT AAG AGG TGA ACA-3′. A 200-bp PCR product represents the wild-type mice; and a 350-bp band represents the deletion of the *pdgf-c* gene. Western blotting shows the absence of the 25-kDa band of the processed PDGF-CC protein in the lungs of the *pdgf-c*–deficient mice (Fig. S1*A*).

Mode ofl Hyaloid Blood Vessel Degeneration and Vessel Analysis. Hyaloid blood vessel regression assays were performed using *pdgf-c*–deficient and wild-type mice as described (2, 4, 5). Briefly, the mouse eyes were enucleated and fixed with 4% (wt/vol) paraformaldehyde (PFA) for 30 min. The eyes then were injected with about 3 μL of 1.5% (wt/vol) low-melting-point agarose (Sigma) in PBS from the optical nerve side into the vitreous. After 30 min at room temperature, the eyeballs were incised around the equator. The hyaloid vessels embedded in agarose were removed from the retinal cup, heated on a glass slide, washed with PBS, and processed for DAPI staining. Vessel number was quantified using previously described methods (5). A circle with a radius of half the maximum radius of the preparation was drawn on the spread of the hyaloid vasculature, and the number of vessels crossing the circle was counted.

Analysis of Blood Vessel Branch Points and Width in *pdgf-c*–Deficient/Wild-Type Mice Using Retinal Whole Mounts. Retinal blood vessels were analyzed using published methods (6) with some minor modifications. Specifically, retinal vessel profiles of *pdgf-c*–deficient and wild-type mice at P15 were determined by IB4 staining using retinal whole mounts or cross-sections. To assess the density of the retinal vascular network using the IB4-stained retinal whole mounts, the number of blood vessel branch points in 30,000-μm^2 areas at the center, paracentral, and peripheral regions of the retinae, at four directions perpendicular to each other, were counted as described (6). Six to eight retinae were analyzed in each group, and four directions were analyzed for each retina. For each direction, three areas were chosen. For the analysis of retinal blood vessel width, 10 random blood vessels were chosen for width measurement in each area, and the average width was calculated; that is, we measured 10 vessels per area, in three areas per direction, in four directions per retina, and there were six to eight retinae per group. The central retinal veins and arteries were excluded.

Analysis of Blood Vessel Density in *pdgf-c*–Deficient and Wild-Type Mice Using Retinal Cryosections. The mouse eyes were embedded in optimum cutting temperature (OCT) compound (Leica) with the 9 and 12 o'clock positions of the corneal limbus facing two marker lines in the embedding container. The whole eye was cryosectioned throughout in parallel with the 12 o'clock meridian, and all the sections were collected. The section on which the optic nerve was visible was used for analysis to ensure that similar positions of the eyes were analyzed. The sections were stained with IB4. For each section, $IB4^+$ vessels were counted in four different locations: at 75% (location 1) and 25% (location 2) of the distance between the optic nerve and the inferior end of the retina and at 25% (location 3) and 75% (location 4) of the distance between the optic nerve and the superior end of the retina. For each retinal section, the four locations first were identified under low magnification, and then an image of a defined microscopic field (425 × 425 μm) was taken under a higher magnification at each location. When images were taken, the retina was adjusted to be in parallel with the bottom line of the microscopic field so that the same amount of retinal tissue (the whole retinal layer, 425 μm in length) was included in each field.

Effect of PDGF-CC on Heme Oxygenase-1 Expression and Blocking of PDGF-CC/PDGFR-α Signaling in the Retinae in Vivo. At P7, C57BL6 neonatal mice were injected intravitreally with PDGF-CC (500 ng per eye; 100-00CC, PeproTech) with or without neutralizing antibodies against PDGF-CC (2 μg per eye; AF1447, R&D) or PDGFR-α (2 μg per eye; AF1062, R&D). The same amount of BSA or goat IgG was used as controls. The mice subsequently were subjected to 75% oxygen for 5 d, and the retinae were harvested at P12 for analysis of heme oxygenase-1 (HMOX1) expression using real-time PCR and immunoprecipitation (IP) followed by immunoblotting (IB) to verify whether at the selected concentrations of both antibodies blocked PDGF-CC/PDGFR-α signaling.

Measurement of Blood Vessel Degeneration, Retinal Thickness, and Vessel Density in rd1 Mice. rd1 (FVB/NJ) mice, in which retinal and retinal blood vessel degeneration occur, are commonly used as a model for retinitis pigmentosa (7). Intravitreal injection of

PDGF-CC protein (500 ng per eye) was performed every 4 d, on P9, P13, P17, and P21, and the retinae were harvested at P25 for analysis. The same amount of BSA was used as a control. To measure retinal thickness, the eyes were embedded and cryosectioned throughout in parallel with the 12:00 o'clock meridian. The sections were used for H&E and immunofluorescence staining. The sections in which the optic nerve was visible were used for analysis. Retinal thickness was measured at four different locations: at 75% (location 1) and 25% (location 2) of the distance between the optic nerve and the inferior end of the peripheral retina and at 25% (location 3) and 75% (location 4) of the distance between the optic nerve and the superior end of the retina. The thickness of the different retinal layers, including the inner nuclear layer and the outer nuclear layer, was measured under 200× magnification. To evaluate vascular density, vascular endothelial cells (ECs) in cryosections were labeled with IB4 and counted as described above. In addition, the superficial, intermediate, and deep layers of retinal blood vessels in the whole mounts (shown in green, red, and blue, respectively) were photographed using a Z1 Imager microscope (Carl Zeiss). Blood vessel density was analyzed using ImageJ software and was defined as the percentage of the total retinal area occupied by blood vessels and their lumens.

Cell Culture, Cell-Survival Assay, and HMOX1 Knockdown by siRNA. Human retinal endothelial cells (HREC), human umbilical vein endothelial cells (HUVEC), human brain vascular smooth muscle cells (HBVSMC), human umbilical vein smooth muscle cells (HUVSMC), and human aortic smooth muscle cells (HASMC) were purchased from ScienCell and were cultured according to the supplier's instructions. Cells between passages 3 and 8 were used for experiments. The immortalized human dermal microvascular endothelial cells (HMEC-1) were cultured in endothelial cell complete medium (ScienCell) consisting of 5% FBS, 1% endothelial cell growth supplement, and 1% penicillin/streptomycin solution. For the cell survival assay, the cells were plated onto 96-well assay plates at different cell densities depending on cell type. At a confluence of 60–70%, the cells were starved and cultured in serum-free medium. Then the 3-[4,5-dimethylthiazol-2-yl]-2,5-diphenyltetrazolium bromide] (MTT) cell viability assay was performed as described (2, 8). PDGF-CC protein (50 or 100 ng/mL) with or without the HMOX1 inhibitor zinc protoporphyrin IX (ZnPP IX) (1 μM or 5 μM) or HMOX1 siRNA (siRNActrl, siRNA1, siRNA2; RiboBio Co. Ltd.) was used in the experiments.

HMOX1 siRNA Knockdown in Cultured Cells in Vitro. HMOX1 siRNAs were transfected into the cells with Lipofectamine RNAiMAX (Invitrogen) according to the manufacturer's protocols. In brief, 30 pmol of control siRNA or HMOX1 siRNA (siRNA1, siRNA2) was mixed with 9 μL of RNAiMAX in Opti-MEM medium and incubated for 15 min at room temperature to allow the complex formation. The complex then was added into each well of six-well plates containing cells in complete culture medium, and cells were incubated for 48–72 h. For siRNA knockdown efficiency, cells were lysed in RIPA lysis buffer, and the protein concentration was determined by Bradford assay. Protein concentrations were normalized, and SDS/PAGE was performed, followed by Western blotting. After starvation in serum-free medium, the HRECs, HUVECs, HBVSMCs, and HUVSMCs were treated with the effective HMOX1 siRNAs with or without 100 ng/mL of PDGF-CC protein, and the MTT cell viability assay performed as described.

PDGFR-α and PDGFR-β Phosphorylation Assay. The PDGFR-α and PDGFR-β activation assay was performed as described (9). Briefly, cultured cells were stimulated with recombinant human PDGF-CC protein at 100 ng/mL for 10, 15, or 30 min. Cell lysates were subjected to further analysis. For the IP assay, cell lysates or retinal lysates were incubated with an anti–PDGFR-α (sc-338; Santa Cruz Biotechnology) or an anti–PDGFR-β antibody (sc-432; Santa Cruz Biotechnology) overnight at 4 °C and were precipitated with anti-rabbit IgG (whole antibody) agarose (Sigma). Immunoprecipitated samples were separated on a 10% SDS/PAGE gel and transferred to a PVDF membrane, which subsequently was incubated with an anti-phosphotyrosine antibody (pY99; Santa Cruz Biotechnology). The second antibody included an HRP-conjugated donkey anti-mouse IgG or an HRP-conjugated donkey anti-rabbit IgG (Dako). Membranes were developed using an enhanced chemiluminescent Western blot substrate (Pierce-Thermo Fisher Scientific Inc.).

HMOX1 Western Blot. When the HBVSMC and HMEC-1 cells were about 80% confluent, the cells were stimulated with 50 ng/mL PDGF-CC for 6 or 24 h, using BSA as a control. The cells then were harvested for HMOX1 analysis using Western blot with a rabbit monoclonal HMOX1 antibody (ab68477; Abcam). The retinae lysate from wild-type or *pdgf-c*–deficient mice at P12 also was harvested for HMOX1 analysis. The second antibody for Western blot was HRP-conjugated donkey anti-rabbit IgG (Dako).

Immunofluorescence Staining. Immunofluorescence staining was performed as described (1, 2, 8, 10). Tissue cryosections or slides of cultured cells were fixed in 4% (wt/vol) PFA for 15 min, permeated with 0.5% Triton X-100 in PBS for 10 min, and blocked with 1% BSA in PBS for 1 h at room temperature and then were incubated in the primary antibody overnight at 4 °C. The antibodies used were anti–PDGFR-α (sc-338; Santa Cruz Biotechnology), anti–PDGFR-β (sc-432; Santa Cruz Biotechnology), anti–p-PDGFR-α (sc-12910; Santa Cruz Biotechnology), anti–p-PDGFR-β (sc-12907; Santa Cruz Biotechnology), anti-IB4 (Invitrogen) or anti-CD31 (BD Biosciences), anti-neural/glial antigen 2 (NG2) (Millipore), and anti- smooth muscle actin (SMA) (M0851; Dako). Corresponding secondary antibodies then were incubated for 1 h. DAPI (Sigma) was used for nuclear staining. Sections were analyzed using a confocal Z1 Imager microscope (Carl Zeiss).

Real-Time PCR. Real-time PCR was performed as described (1, 2, 9) using the primers listed in Table S1.

1. Hou X, et al. (2010) PDGF-CC blockade inhibits pathological angiogenesis by acting on multiple cellular and molecular targets. *Proc Natl Acad Sci USA* 107(27):12216–12221.
2. Zhang F, et al. (2009) VEGF-B is dispensable for blood vessel growth but critical for their survival, and VEGF-B targeting inhibits pathological angiogenesis. *Proc Natl Acad Sci USA* 106(15):6152–6157.
3. Ding H, et al. (2004) A specific requirement for PDGF-C in palate formation and PDGFR-alpha signaling. *Nat Genet* 36(10):1111–1116.
4. Lobov IB, et al. (2005) WNT7b mediates macrophage-induced programmed cell death in patterning of the vasculature. *Nature* 437(7057):417–421.
5. Kato M, et al. (2002) Cbfa1-independent decrease in osteoblast proliferation, osteopenia, and persistent embryonic eye vascularization in mice deficient in Lrp5, a Wnt coreceptor. *J Cell Biol* 157(2):303–314.
6. Hellström M, et al. (2007) Dll4 signalling through Notch1 regulates formation of tip cells during angiogenesis. *Nature* 445(7129):776–780.
7. Otani A, et al. (2002) Bone marrow-derived stem cells target retinal astrocytes and can promote or inhibit retinal angiogenesis. *Nat Med* 8(9):1004–1010.
8. Li Y, et al. (2008) VEGF-B inhibits apoptosis via VEGFR-1-mediated suppression of the expression of BH3-only protein genes in mice and rats. *J Clin Invest* 118(3): 913–923.
9. Tang Z, et al. (2010) Survival effect of PDGF-CC rescues neurons from apoptosis in both brain and retina by regulating GSK3beta phosphorylation. *J Exp Med* 207(4): 867–880.
10. Zhang F, et al. (2012) Proliferative and survival effects of PUMA promote angiogenesis. *Cell Reports* 2(5):1272–1285.

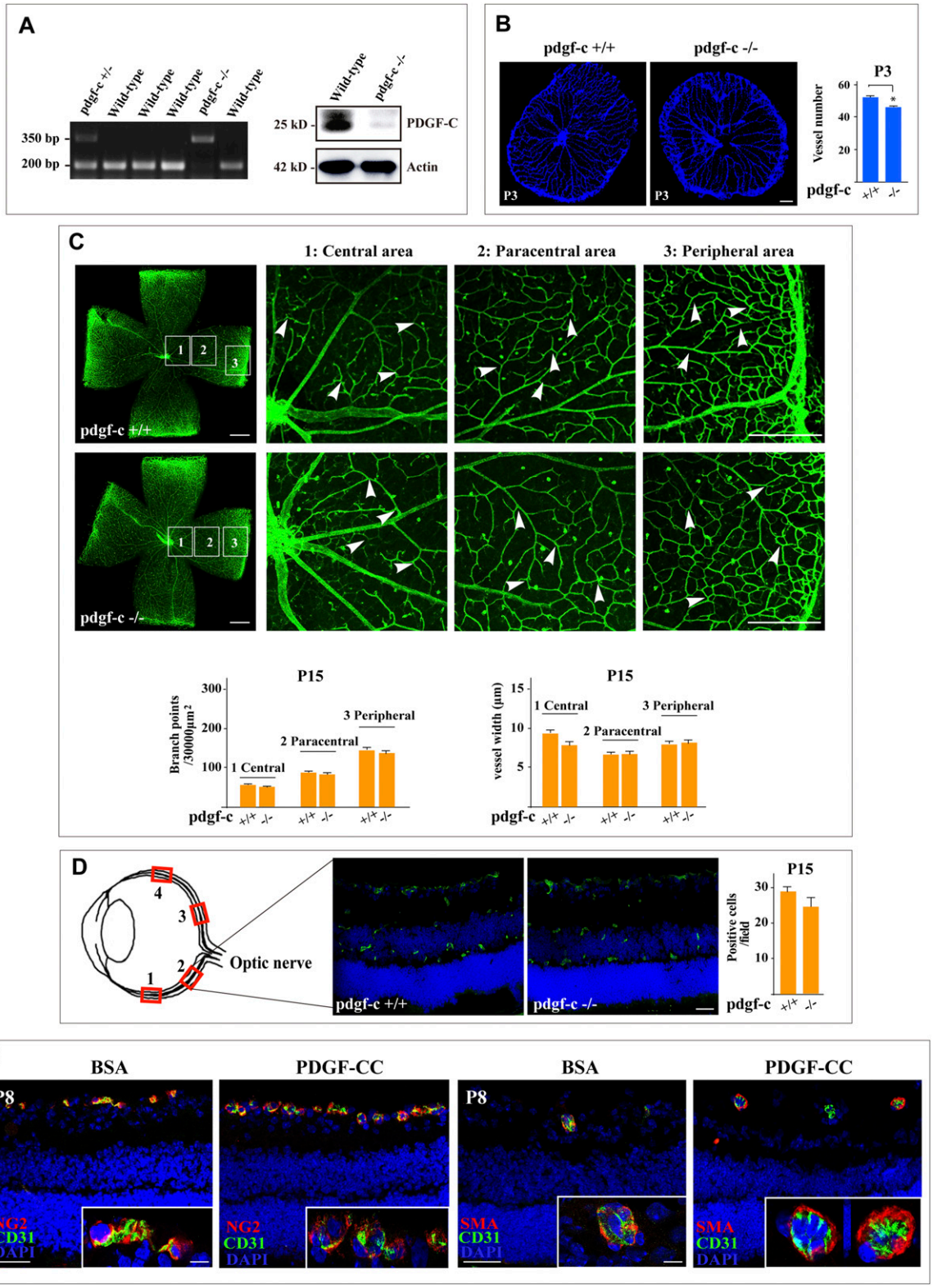

Fig. S1. *pdgf-c* deficiency accelerates hyaloid blood vessel regression, whereas PDGF-CC treatment rescues retinal blood vessels from regression in an OIR model. (*A*, *Left*) Genotyping analyses by PCR showed the deletion of the *pdgf-c* gene by a 350-bp band and the presence of the *pdgf-c* gene by a 200-bp band. (*Right*) Western blot showed the lack of the proteolytically processed 25-kDa PDGF-C band in the lungs of *pdgf-c* knockout mice. (*B*) *pdgf-c* deficiency accelerated the regression of hyaloid blood vessels, leading to lower hyaloid vessel density at P3. (*C*) IB4 staining of whole-mount retinae showed no significant difference in the number of vessel branch points and vessel width between wild-type and *pdgf-c*–deficient mice in the central, paracentral, and peripheral retinae at P15. (*D*, *Right*) A schematic presentation of the positions analyzed on the retinal whole mounts with IB4 staining. (*Left*) No significant difference in retinal blood vessel density between wild-type and *pdgf-c*–deficient mice at P15 was found. (*E*) Immunofluorescent staining using EC, pericyte, and smooth muscle cell markers showed that 24 h after hyperoxia at P8, PDGF-CC treatment rescued retinal blood vessels from regression in an OIR model and resulted in more $CD31^+$, $NG2^+$, or SMA^+ blood vessels. (Scale bars: 200 μm in *B*; 300 μm in *C*; 20 μm in *D*; 50 μm in *E*; 10 μm in *E Insets*.) $^*P < 0.05$.

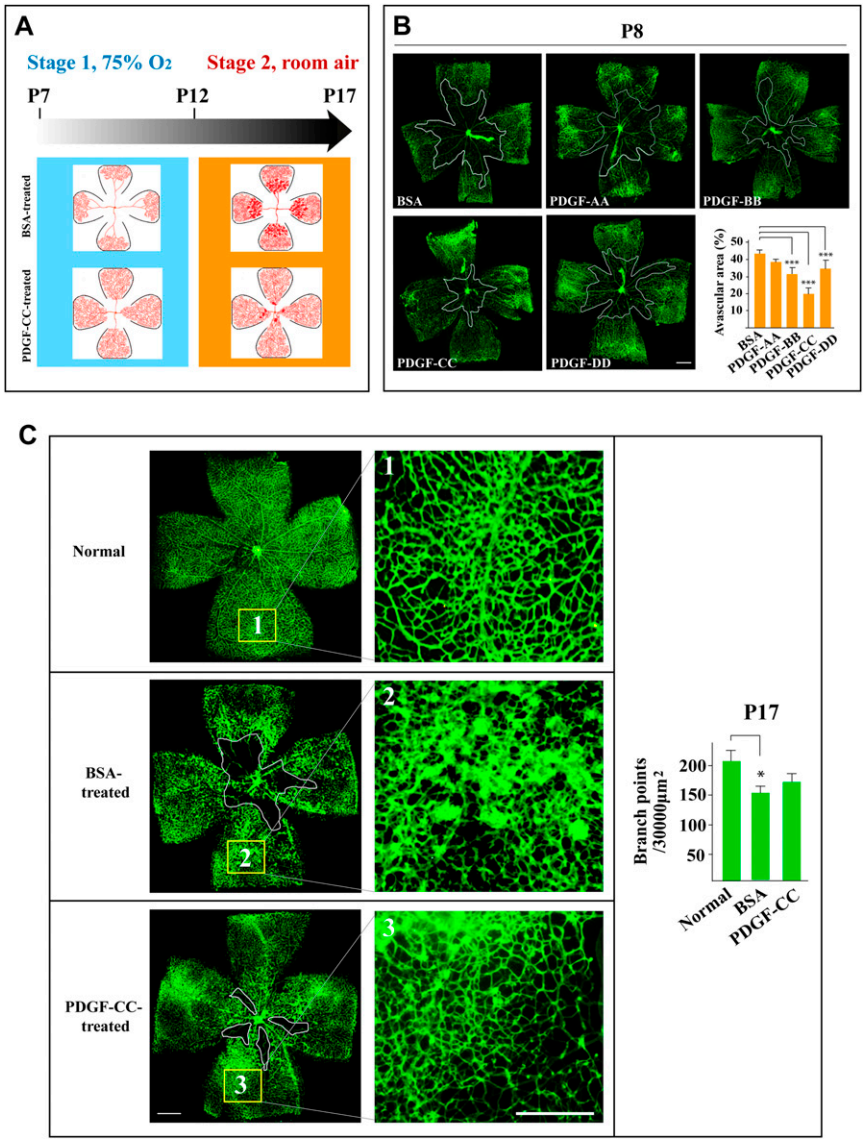

Fig. S2. PDGF-CC rescued the retinal blood vessels from regression in a model of hyperoxia-induced vessel degeneration. (*A*) The OIR model includes two stages. In the first stage (75% O_2), hyperoxia induces retinal blood vessel regression from P7 to P12. In the second stage (room air), blood vessel regression leads to retinal hypoxia, which results in retinal neovascularization peaking at P17. Therefore, if a potent vasoprotective factor were supplied in the first stage to prevent retinal blood vessels from regressing, there would not be subsequent retinal neovascularization in the second stage. (*B*) In a model of hyperoxia-induced retinal blood vessel degeneration, intravitreal injection of PDGF-CC protein rescued retinal blood vessels from regression after 1 d of hyperoxia at P8, leading to smaller avascular areas than seen in BSA-treated retinae. PDGF-BB and PDGF-DD displayed some effect. PDGF-AA had no effect. (*C*) As compared with normal P17 retinal blood vessels (*Top*), PDGF-CC treatment (*Bottom*) did not lead to more blood vessels than seen in normal retinae. PDGF-CC treatment promoted retinal blood vessel regrowth leading to a smaller avascular area and hypoxia-induced neovascularization as compared with BSA treatment (*Middle*). Images of higher magnification show relatively well-organized revascularization in the retinae treated with PDGF-CC, whereas retinae treated with BSA display irregular, tortuous, and clustering neovascular tufts. (Scale bars: 300 μm.) $*P < 0.05$, $***P < 0.001$.

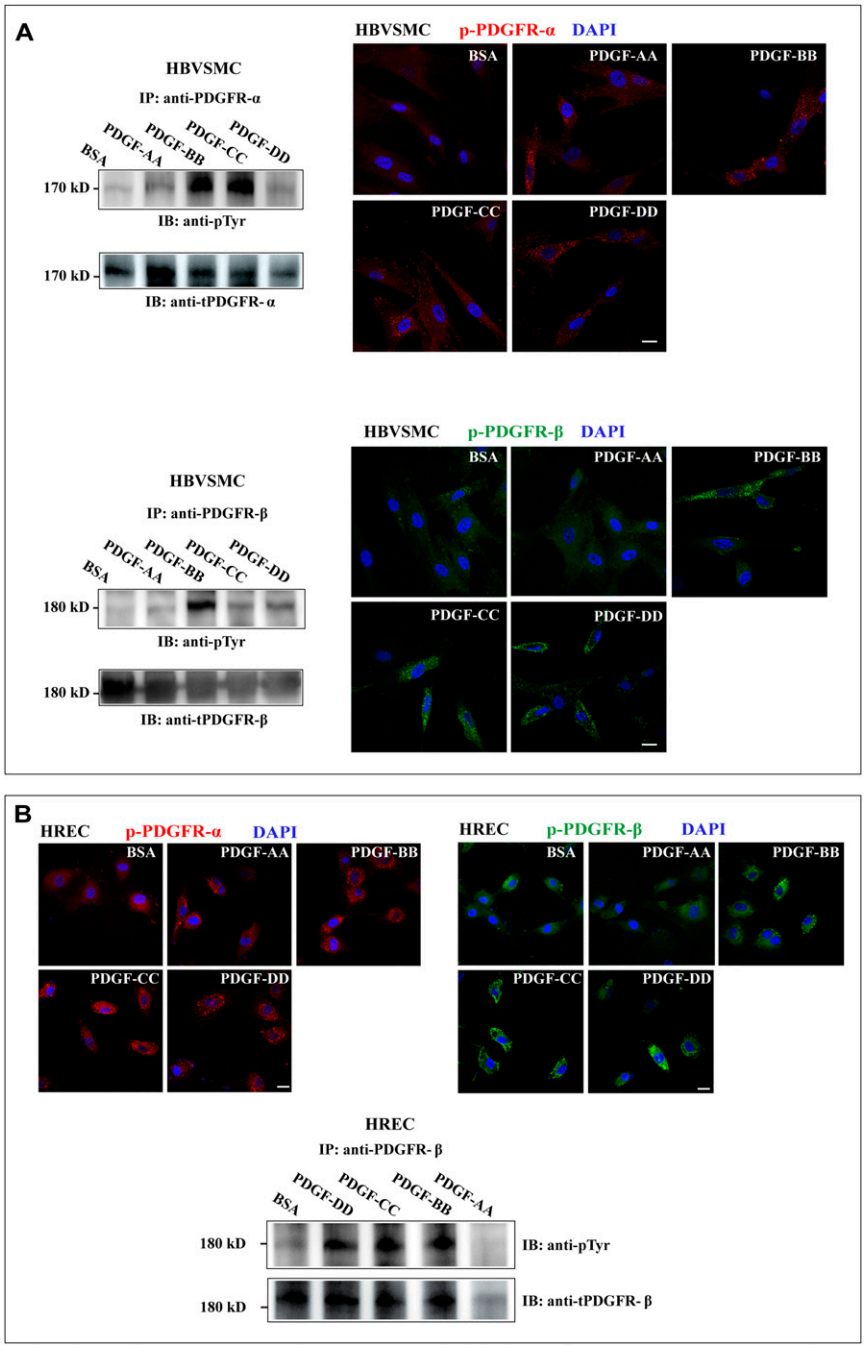

Fig. S3. PDGFs activated PDGFR-α and PDGFR-β in SMCs and ECs. (*A*, *Left*) IP followed by IB detected respective PDGFR-α and PDGFR-β activation by PDGF-AA, PDGF-BB, PDGF-CC, and PDGF-DD (50 ng/mL each) in HBVSMCs. (*Right*) Immunofluorescent staining detected respective phosphorylated PDGFR-α (red) and phosphorylated PDGFR-β (green) in HBVSMCs treated with PDGF-AA, PDGF-BB, PDGF-CC, and PDGF-DD (50 ng/mL each). (*B*, *Upper*) Immunofluorescent staining detected respective phosphorylated PDGFR-α (red) and phosphorylated PDGFR-β (green) in HRECs treated with PDGF-AA, PDGF-BB, PDGF-CC, and PDGF-DD. (*Lower*) IP followed by IB revealed PDGFR-β activation by PDGF-BB, PDGF-CC, and PDGF-DD. (Scale bars: 20 μm.)

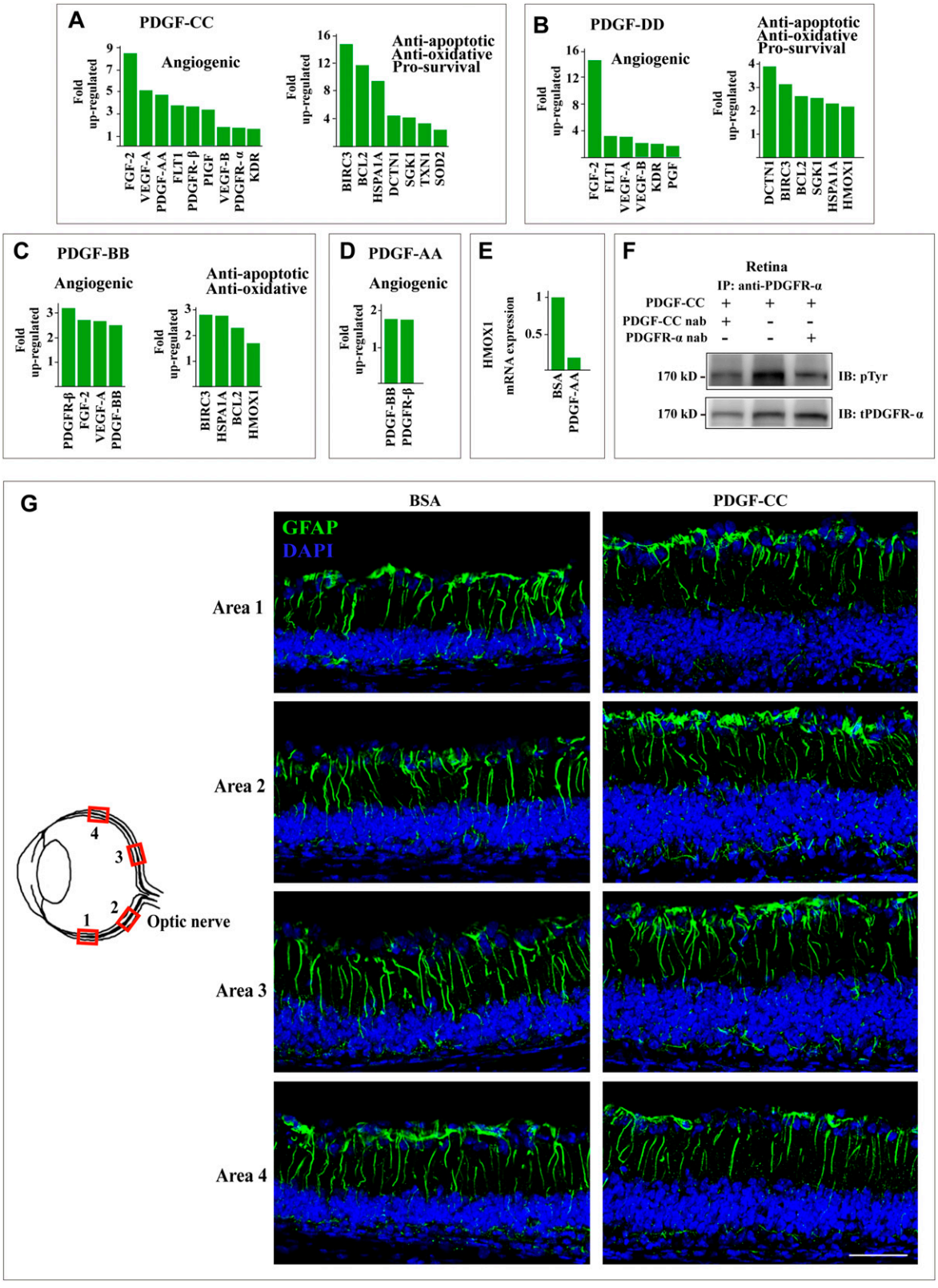

Fig. S4. PDGF-CC up-regulated the expression of prosurvival, antiapoptotic, antioxidative, and angiogenic genes in vivo. (*A*) Real-time PCR showed that PDGF-CC treatment up-regulated the expression of many prosurvival, antiapoptotic, antioxidative, and angiogenic genes in retinae 24 h after hyperoxia. (*B* and *C*) PDGF-DD (*B*) and PDGF-BB (*C*) had some effect. (*D*) PDGF-AA had no effect on the expression of the prosurvival, antiapoptotic, antioxidative gene (not shown) but modestly increased the expressions of PDGF-BB and PDGFR-β. (*E*) PDGF-AA down-regulated HMOX1 expression in the retinae 24 h after hyperoxia shown by real-time PCR. (*F*) IP followed by IB showed that PDGF-CC and PDGFR-α neutralizing antibodies inhibited PDGFR-α activation in the retinae in vivo in an OIR model. nab, neutralizing antibody. (*G*, *Left*) A schematic presentation shows the locations analyzed on retinal cryosections. (*Right*) GFAP staining showed no significant difference in glial activation between BSA- and PDGF-CC–treated retinae of rd1 mice. (Scale bar: 50 μm.)

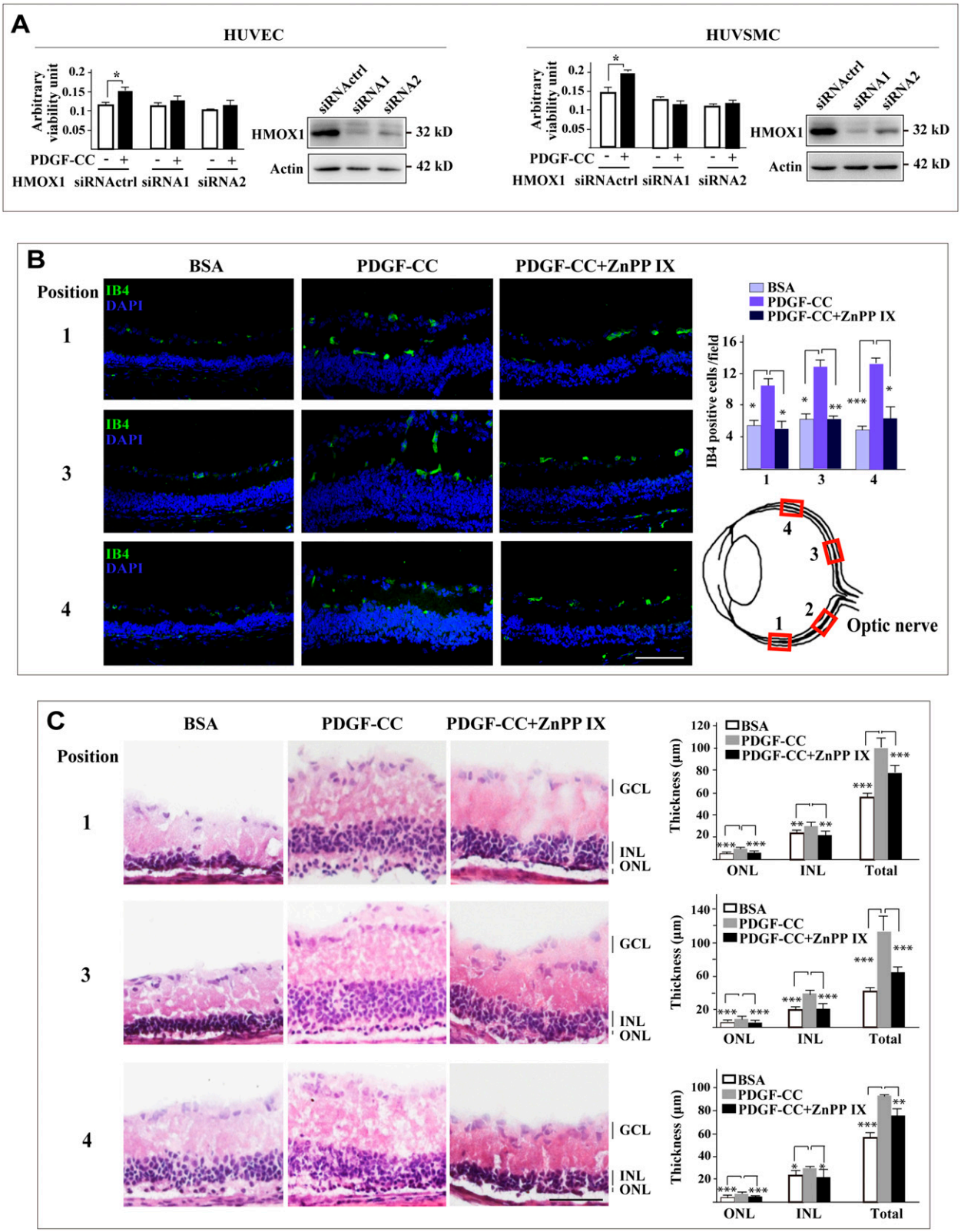

Fig. S5. HMOX1 mediates the vasoprotective effect of PDGF-CC in vitro and in vivo. (*A*) PDGF-CC treatment increased survival of HUVECs and HUVSMCs cultured in serum-free medium. Knockdown of HMOX1 by siRNA abolished the survival effect of PDGF-CC. Decreased HMOX1 protein level after HMOX1 siRNA transfection was confirmed by Western blot. (*B*) In a retinitis pigmentosa model (rd1 mice), IB4 staining showed that intravitreal injection of PDGF-CC protein rescued retinal blood vessels from degeneration and resulted in higher blood vessel densities. The effect of PDGF-CC was abolished almost completely by a HMOX1 inhibitor, ZnPP IX. (*C*) H&E staining showed severe retinal degeneration in the BSA-treated retinae of rd1 mice (retinitis pigmentosa model). PDGF-CC protein treatment rescued the retinae from degeneration and markedly increased the thickness of retinal layers, including the inner nuclear layer (INL) and the outer nuclear layer (ONL). The rescue effect of PDGF-CC was abolished almost completely by a HMOX1 inhibitor, ZnPP IX. GCL, ganglion cell layer. (Scale bars: 50 μm.) $*P < 0.05$, $**P < 0.01$, $***P < 0.001$.

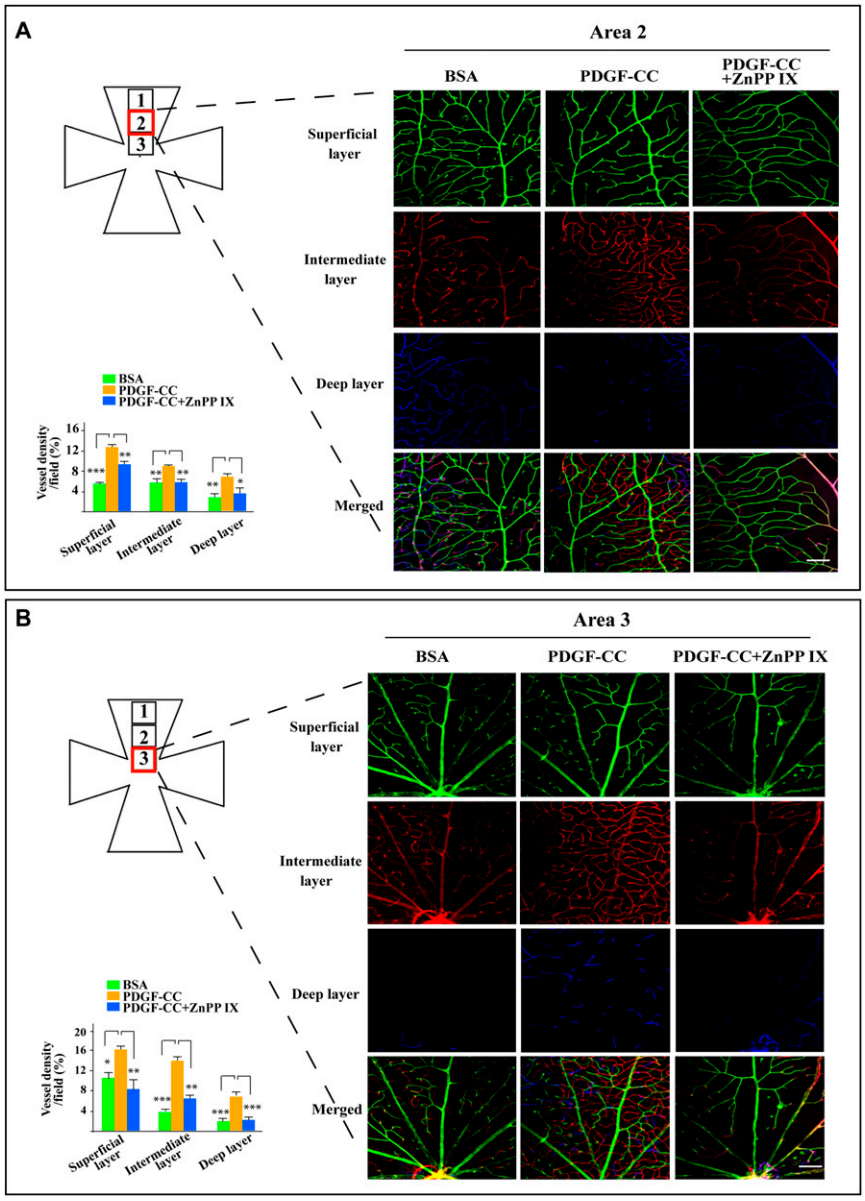

Fig. S6. PDGF-CC rescued retinal blood vessel degeneration via HMOX1 in a retinitis pigmentosa model. (*Right*) Schematic presentation of the positions analyzed on whole-mount retinae. In a retinitis pigmentosa model (rd1 mice), IB4 staining showed that intravitreal injection of PDGF-CC protein rescued the degeneration of different layers of retinal blood vessels in the paracentral (*A*) and central (*B*) areas. The effect of PDGF-CC was abolished almost completely by a HMOX1 inhibitor, ZnPP IX. (Scale bars: 100 μm.) $*P < 0.05$, $**P < 0.01$, $***P < 0.001$.

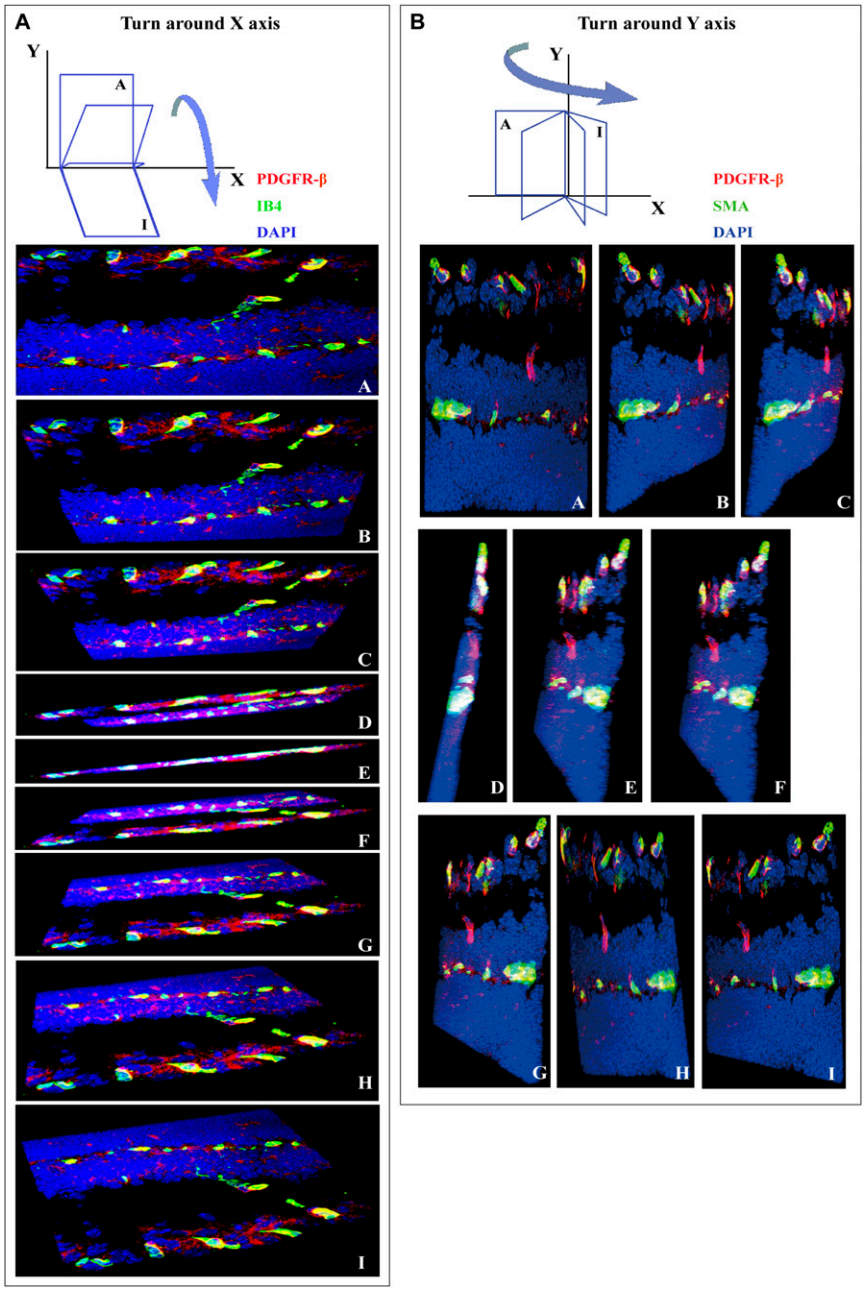

Fig. S7. PDGFR-β is expressed by retinal vascular ECs and vascular smooth muscle cells. (*A*) Continuous confocal images turning around the *x* axis (subpanels *A–I*) of immunofluorescence staining using retinal cryosections from P12 mice showed that PDGFR-β expression (red) was colocalized with the $IB4^+$ ECs (green) throughout the retinae. (*B*) Continuous confocal images turning around the *y* axis (subpanels *A–I*) of immunofluorescence staining showed that PDGFR-β expression (red) was colocalized with SMA^+ smooth muscle cells (green) throughout the retinae.

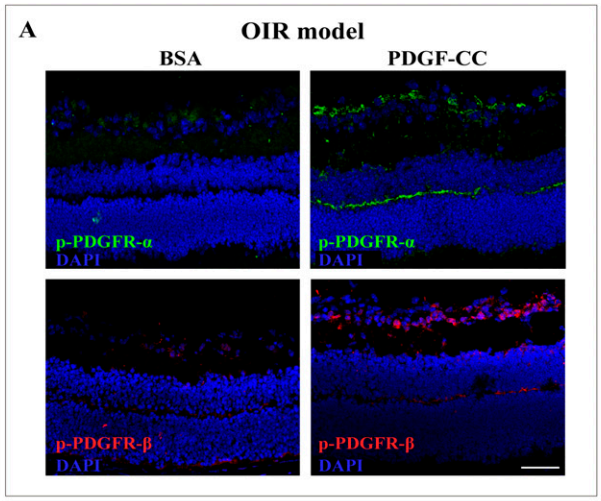

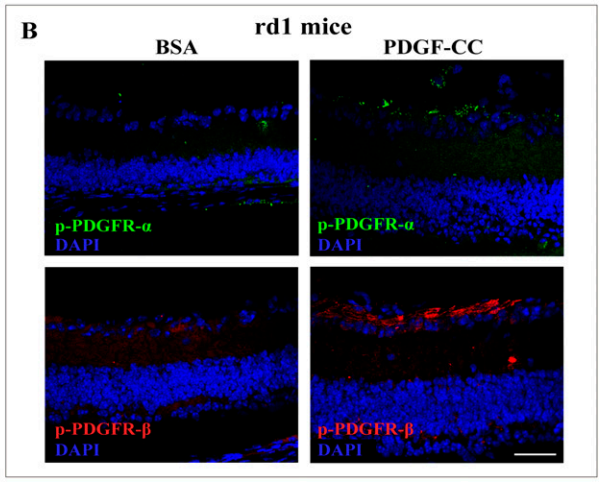

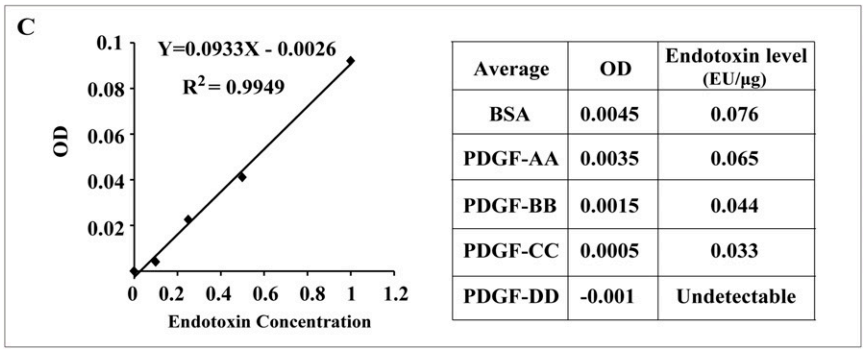

Average	OD	Endotoxin level (EU/μg)
BSA	0.0045	0.076
PDGF-AA	0.0035	0.065
PDGF-BB	0.0015	0.044
PDGF-CC	0.0005	0.033
PDGF-DD	-0.001	Undetectable

Fig. S8. PDGFR-α and PDGFR-β are activated by PDGF-CC in vivo. (*A*) In an OIR model, immunofluorescent staining using antibodies against phosphorylated PDGFR-α and PDGFR-β detected activated PDGFR-α (green) and PDGFR-β (red) mainly in the ganglion cell layer and outer plexiform layer of the retinae after PDGF-CC treatment. (*B*) In a retinitis pigmentosa model (rd1 mice), intravitreal injection of PDGF-CC protein activated PDGFR-α and PDGFR-β in the retinae. (*C*) Endotoxin levels in PDGF-AA, PDGF-BB, PDGF-CC, and PDGF-DD proteins were measured using an endotoxin detection kit. The standard curve is shown on the left, and the results are shown on the right. Endotoxin levels in all of the proteins are less than 0.1 EU/μg. (Scale bars: 50 μm.)

Table S1. Primers used for real-time PCR

Gene	Orientation	Primer sequence (5′ to 3′)
hmox1	Forward	GAAGGAGGCCACCAAGGAG
	Reverse	GGTCACCCAGGTAGCGGG
fgf2	Forward	CAACCGGTACCTTGCTATGA
	Reverse	TCCGTGACCGGTAAGTATTG
vegf-a	Forward	CACAGCAGATGTGAATGCAG
	Reverse	TTTACACGTCTGCGGATCTT
pdgf-a	Forward	CTCTTGGAGATAGACTCCGTAGG
	Reverse	ACTTCTCTTCCTGCGAATGG
flt1	Forward	GCTCTGATGACCGAACTCAA
	Reverse	ATTCCACGATCACCATCAGA
pdgfr-β	Forward	AGCCAGAAGTAGCGAGAAGC
	Reverse	GGCAGTATTCCGTGATGATG
plgf	Forward	CCTCTAAAAGAAGTTCATTGTC
	Reverse	GTCTTTCCCAATCCAGTGG
vegf-b	Forward	TGACATCATCCATCCCACTC
	Reverse	CCTTGGCAATGGAGGAAG
pdgfr-α	Forward	TCAGAGAGTTCGTGGTGGAG
	Reverse	ATCAGTGGTGATCTCGGTGA
kdr	Forward	TTGTAAACCGGGATGTGAAA
	Reverse	TTCTCTTGATCATCCGTCCA
birc3	Forward	TGTCAGCCAAGTTCAAGCTG
	Reverse	ATCTTCCGAACTTTCTCCAGGG
bcl2	Forward	ACTTCTCTCGTCGCTACCGT
	Reverse	TCCCTGAAGAGTTCCTCCAC
hspa1a	Forward	ACAAGAAGAAGGTGCTGGACA
	Reverse	CTGGTACAGCCCACTGATGAT
dctn1	Forward	GGAAGAGCAGCAAGATGACA
	Reverse	TAGGAGATGAGGCGACTGTG
sgk1	Forward	TTCCTTACCCTTTGGTGGAG
	Reverse	GAGAGGAGGGTGTGCTCTTC
txn1	Forward	GATGGGGTCTCGGAGGAAC
	Reverse	GTAAGGCAAGGAGAAAAGATC
sod2	Forward	CAGATCATGCAGCTGCACC
	Reverse	CATTCTCCCAGTTGATTACATTC
pdgf-b	Forward	ATCCGCTCCTTTGATGATCT
	Reverse	GAGCTTTCCAACTCGACTCC
pdf	Forward	CTCTCTGGAACACAGGCAGA
	Reverse	CCGTAGCTGTACCACGAAGA
actb	Forward	AGTGTGACGTTGACATCCGT
	Reverse	TGCTAGGAGCCAGAGCAGTA

All genes were expressed in mouse.